Journal of Maps

ISSN: (Print) 1744-5647 (Online) Journal homepage: https://www.tandfonline.com/loi/tjom20

Structural and petrographic map of the Sassa gabbro complex (Dent Blanche nappe, Austroalpine tectonic system, Western Alps, Italy)

Luca Baletti , Davide Zanoni , M. Iole Spalla & Guido Gosso

To cite this article: Luca Baletti , Davide Zanoni , M. Iole Spalla & Guido Gosso (2012) Structural and petrographic map of the Sassa gabbro complex (Dent Blanche nappe, Austroalpine tectonic system, Western Alps, Italy), Journal of Maps, 8:4, 413-430, DOI: 10.1080/17445647.2012.745678

To link to this article: https://doi.org/10.1080/17445647.2012.745678

Journal of Maps
Vol. 8, No. 4, December 2012, 413–430

Routledge
Taylor & Francis Group

SCIENCE

Structural and petrographic map of the Sassa gabbro complex (Dent Blanche nappe, Austroalpine tectonic system, Western Alps, Italy)

Luca Baletti[a], Davide Zanoni[a]*, M. Iole Spalla[a,b] and Guido Gosso[a,b]

[a]*Dipartimento di Scienze della Terra 'A. Desio', Università degli Studi di Milano, Via Mangiagalli 34, 20133 Milano, Italy;*
[b]*C.N.R. – Istituto per la Dinamica dei Processi Ambientali, Via Mangiagalli 34, 20133 Milano, Italy*

(*Received 20 January 2012; Resubmitted 3 September 2012; Accepted 24 October 2012*)

The Sassa gabbro complex outcrops in the upper Valpelline and is part of the Permian gabbros of the Collon – Matterhorn group, set in the Dent Blanche nappe of the Western Austroalpine tectonic system. This 1:2500-scale map was constructed through the synergic use of meso- and microscopic analysis of fabrics to identify the relationships of the superposed foliations with the growth of equilibrium mineral assemblages. Throughout the foliation trajectories, a mosaic of rock volumes, in which strain is differently partitioned, is highlighted on the map for all the successive deformation stages. Therefore, this mosaic shows deformation gradients spanning from unstrained or weakly strained domains, where the primary magmatic features are still well preserved, to domains in which the Alpine fabrics are pervasive and obliterate the previous structures. The pre-Alpine history is characterized by the polyphasic emplacement of the Sassa gabbro and by a coronitic growth of successive mineral assemblages during crustal thinning-related exhumation. The Alpine history is characterized by multistage heterogeneous deformation consisting of a first D1 stage developed in blueschist facies conditions followed by D2 and D3 stages developed in greenschist facies conditions. In summary, by applying this analytical method, the geologic traces of the pre-Alpine lithospheric thinning and Alpine subduction histories have been separated.

Keywords: Permian gabbros; pre-Alpine vs. Alpine evolution; strain partitioning map; multi-scale structural analysis

1. Introduction

The reconstruction of tectonic events and the evolution of thermal history through time in orogens requires high quality structural and petrographic mapping. The resulting geological maps should synthesize: (i) the grids of superposed foliation trajectories with related lineations; and (ii) the mineral assemblages marking successive fabrics, useful to unravel the metamorphic environment, which assists or overprints each deformation event (e.g., Austrheim, 1990; Connors & Lister, 1995; Gosso et al., 1983; Johnson & Duncan, 1992; Spalla, Siletto, Di Paola, & Gosso, 2000; Spalla, Zanoni, Williams, & Gosso, 2011; Williams, 1985; Zanoni, 2010; Zucali, Spalla, & Gosso, 2002). Such maps represent an effective correlation tool for determining structural and metamorphic regional events to identify shape and size of tectonic units (Figure 1) in polydeformed and polymetamorphic terrains (e.g., Salvi, Spalla, Zucali, & Gosso, 2010; Spalla, Gosso, Marotta, Zucali, & Salvi, 2010; Spalla, Zucali, Di Paola, & Gosso, 2005).

This contribution concerns an example from the European Alps that shows this type of mapping applied to an area where a continental crust underwent two superposed tectonic and metamorphic cycles, related to pre-Alpine rifting and Alpine subduction-collision. The map synthesizes lithologic, structural, and metamorphic data, collected at the boundary between a pre-Alpine gabbro body and its country rocks, in the Dent Blanche Nappe (DBN) of the Austroalpine tectonic system (Western Italian Alps).

*Corresponding author. Email: davide.zanoni@unimi.it

ISSN 1744-5647 online

http://dx.doi.org/10.1080/17445647.2012.745678
http://www.tandfonline.com

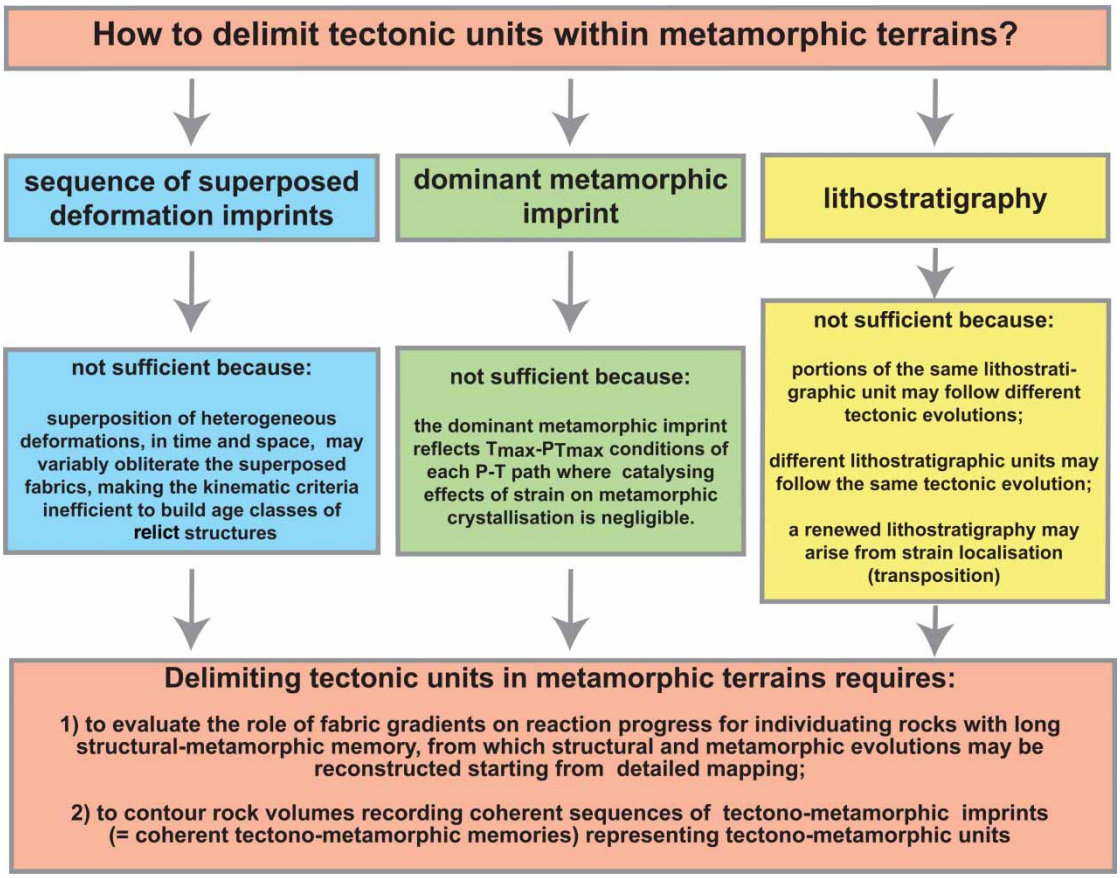

Figure 1. Flow chart showing how to delimit tectonic units in poly-deformed and poly-metamorphic terranes; redrawn after Spalla et al. (2005).

2. Geologic outline

Within the continental crust of the Alps, gabbro bodies mainly occur in the Austroalpine and Southalpine (Adria plate) high temperature metamorphic rocks (Figure 2).

The Austroalpine system is the uppermost continental element tectonically overlying the stack of oceanic and continental nappes of the Alpine suture zone and in the Western Alps consists of the internal Sesia-Lanzo Zone (SLZ) and the external DBN, with related outliers (Dal Piaz, 1999). The Austroalpine system was deformed and metamorphosed from Cretaceous-Paleogene to Eocene-Lower Oligocene under different PT conditions (eclogite to greenschist facies conditions; Ernst & Liou, 2008); this metamorphic evolution, widely recorded in the Western Alps, indicates that the Austroalpine system was deeply implicated in the Alpine subduction-collision processes (Compagnoni et al., 1977; Dal Piaz, Hunziker, & Martinotti, 1972; Gosso, Messiga, Rebay, & Spalla, 2010; Meda, Marotta, & Spalla, 2010; Polino, Dal Piaz, & Gosso, 1990; Spalla, Gosso, Marotta, Zucali, & Salvi, 2010; Zanoni, Spalla, & Gosso, 2010 and refs. therein).

The pre-Alpine protoliths are high metamorphic grade paragneisses (kinzigites, felsic granulites), with interbeddings of mafic granulites, amphibolites, and marbles, Permian intrusive granitoids and gabbros, and minor Mesozoic sedimentary covers (Compagnoni et al., 1977; Dal Piaz, 1993; Manzotti, 2011; Roda & Zucali, 2011; Venturini, Martinotti, Armando, Barbero, & Hunziker, 1994). The DBN, as the rest of the Austroalpine system of Western Alps, is composed of two superposed tectonic elements: an upper element, formed by lower continental crust rocks, known as the Valpelline Series (VS) and a lower element, known as the Arolla Series (AS; Argand, 1911). AS is widespread in the North-Western DBN and is mainly formed by Permian acidic and mafic intrusives, associated with minor high-grade gneisses and metabasics. Slivers of Mesozoic metasediments are pinched along a main shear zone, separating DBN into two main tectonic units (DBN s.s. and Mont Mary) and trending NNE-SSW (Canepa, Castelletto, Cesare, Martin, & Zaggia, 1990); relics of Norian foraminifera and algae have been detected in these metasediments (Ciarapica, Dal Piaz, & Passeri, 2010). The lower continental crust rocks of the upper

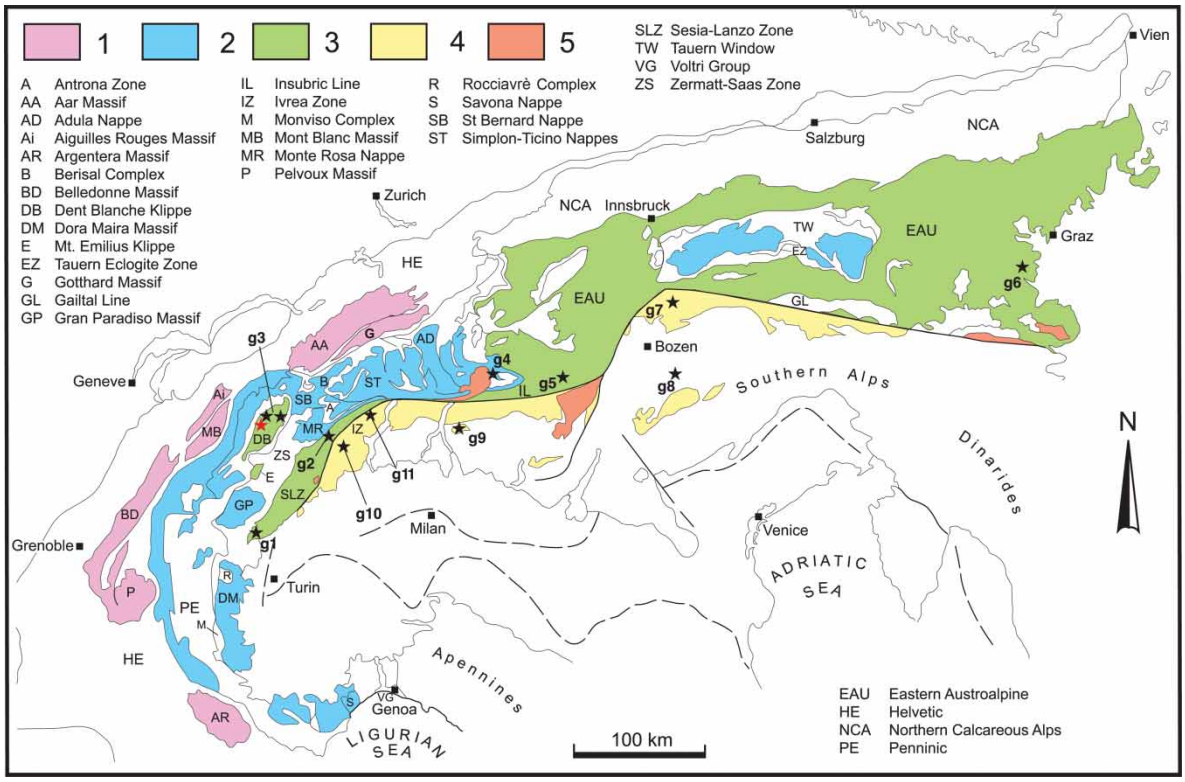

Figure 2. Tectonic sketch map of the Alps; 1 = crystalline massifs of the Helvetic units; 2 = continental Penninic units; 3 = Austroalpine units; 4 = Southalpine crystalline basement units; 5 = Periadriatic Oligocene intermediate to granitic magmatic bodies. Stars = Permian gabbroic bodies in the pre-Alpine continental crust: g1 = Corio – Monastero (SLZ); g2 = Sermenza (SLZ); g3 = Matterhorn – Collon – Sassa (DB); g4 = Fedoz – Braccia; g5 = Sondalo; g6 = Baerofen and Gressenberg; g7 = Bressanone - Chiusa; g8 = Predazzo - Monzoni; g9 = Val Biandino; g10 = Ivrea Val Mastallone; g11 = Ivrea - Finero. The red star locates the Sassa complex.

elements are closely similar to those of the Ivrea Zone (Southern Alps; Figure 2). This affinity suggests that Austroalpine and Southalpine domains were continuous (Adria Alpine hinterland) during Alpine convergence (Canepa et al., 1990; Compagnoni et al., 1977; Diehl, Masson, & Stutz, 1952; Stutz & Masson, 1938; Vuichard, 1989). The pre-Alpine metamorphic evolution was accomplished under a high T/P ratio, associated with gabbro and granitoid emplacement, and widely interpreted as the consequence of a Permian-Triassic lithospheric thinning, heralding the opening of the Tethyan ocean (e.g., Bussy, Venturini, Hunziker, & Martinotti, 1998; Lardeaux & Spalla, 1991; Marotta, Spalla, & Gosso, 2009; Rebay & Spalla, 2001; Roda & Zucali, 2008). Abundant gabbro bodies are mainly hosted in Permian granitoids of the AS; the main complexes are Matterhorn, Collon, and Sassa. Thick mylonitic bands mark the boundaries between the gabbro bodies and country rocks, affecting both rock types (Dal Piaz, De Vecchi, & Hunziker, 1977; Diehl et al., 1952; Monjoie, Bussy, Lapierre, & Pfeifer, 2005; Pennacchioni & Guermani, 1993).

The Alpine metamorphic history of the DBN is less constrained with respect to that of the widely eclogitized SLZ. Where Alpine HP mineral assemblages have been described, both in VS and AS, they indicate metamorphic peak conditions compatible with blueschist facies and interpreted, on the basis of available radiometric data, as 48-45 Ma old (Ayrton, Bugnon, Haarpainter, Weidmann, & Frank, 1982; Canepa et al., 1990; Gardien, Reusser, & Marquer, 1994; Kienast & Nicot, 1971; Pennacchioni & Guermani, 1993; Roda & Zucali, 2008).

3. Mapping and representation techniques

The reconstruction of the sequence of structural and metamorphic imprints affecting poly-deformed and poly-metamorphic terrains is crucial to decipher the tectonics responsible for crustal accretion or consumption. Therefore, maps synthesizing rock associations, the grid of superimposed foliations, and indications of metamorphic

environments in which they developed, constitute a fundamental support for deriving interpretations on tectonics of active margins. Such synthetic mapping is rarely performed and generally the tectonic subdivisions are inferred on the basis of lithostratigraphic and/or dominant metamorphic imprint affinities. Unfortunately, the strong influence of the dominant metamorphic imprint on variations of the lithostratigraphic setting (e.g., Passchier, Myers, & Kröner, 1990) makes this approach inadequate. To infer a more complete tectonic history, this map is therefore an integrated report of the field and laboratory analytical work carried out to reconstruct the relationships between the finite deformation field, metamorphic evolution, and lithostratigraphy. The Sassa gabbro, being an igneous complex recording a polycyclic metamorphic and structural history, and surfacing in a recently deglaciated Alpine area, represents an ideal terrain with a rich lithostratigraphy and superposed structural and metamorphic imprints. On the map the number of dots along trajectory traces indicates timing of superposed planar fabrics. Through micro-scale analysis, the mineral assemblages related to successive fabrics in each rock type are inferred and detailed in the map legend. They represent the basis to identify the metamorphic environment (i.e., metamorphic facies) in which the successive fabrics developed (differently colored trajectories). In this way, information on chronology of structural imprints and metamorphic environment in which they developed are located in space. In addition, strain partitioning generates contemporaneous fabric heterogeneities in adjacent rock volumes (Figure 3) that can be exploited to refine the exploration of the tectono-metamorphic memory of polydeformed rocks (e.g., Hobbs, Ord, Spalla, Gosso, & Zucali, 2010; Salvi et al., 2010 and refs therein): mineral assemblages supporting coronitic, tectonitic, and mylonitic fabrics are here described and compared to achieve this goal.

The Sassa geological map used a topographic base (the CTR - Technical Regional Topography) provided by the Val d'Aosta Regional Administration. The projection coordinate system is UTM ED50; the original 1:10,000-scale was enlarged up to 1:2500 to increase the mapping detail. The map presents a synthesis of the whole data set at a scale of 1:2500 on a redrawn original topographic base. Graphical representation was performed using Adobe Illustrator.

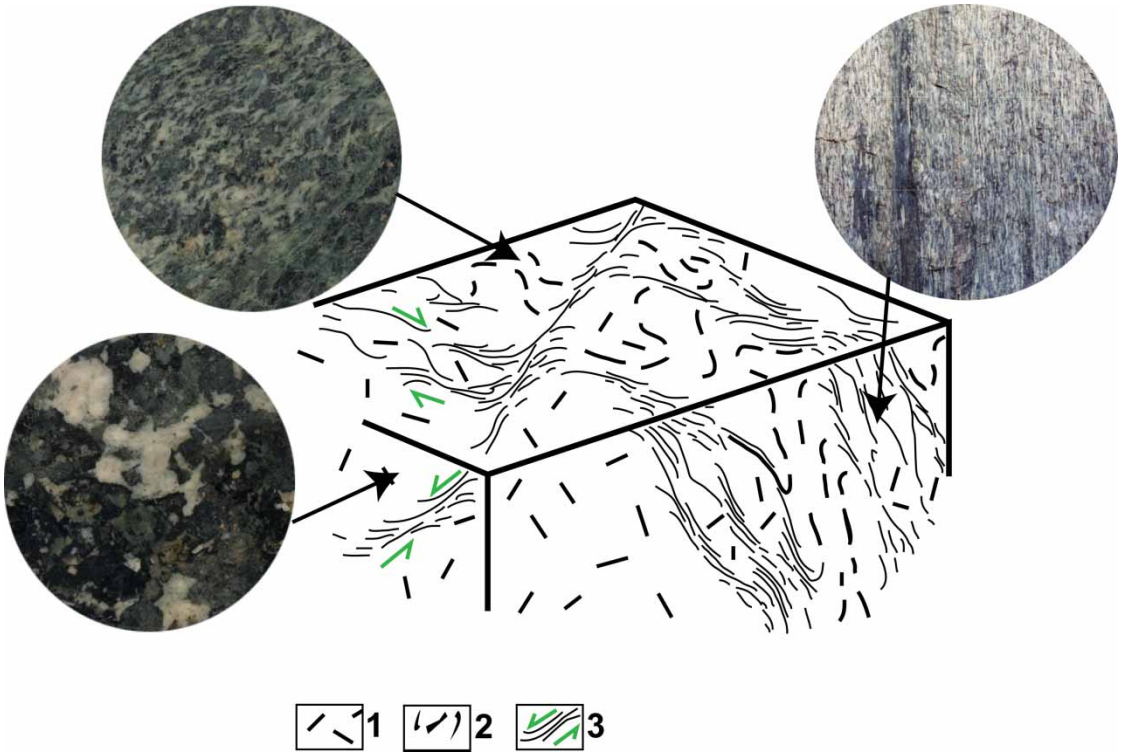

Figure 3. Schematic block diagram showing strain partitioning, generating mylonitic, tectonitic, and coronitic textures, as a consequence of deformation of a homogeneous massive rock volume. The close up shows the corresponding textures of the Sassa gabbro. Legend: 1 = coronite, 2 = tectonite, 3 = mylonite. Redrawn after Lardeaux and Spalla (1990).

The map plate displays equal area lower hemisphere Schmidt projections (StereoWinFull120; Allmendinger, 2002) of superposed fabric elements, such as tectonic (S1, S2, S3) and magmatic foliations, fold axes (B2, B3), and magmatic lineations (n = number of measurements).

Meso- and microstructures of the most significant stages of the geological history of the analyzed area are shown in pictures on the map.

4. Original field data

Structural mapping has been performed in two key subareas of the Sassa complex characterized by different rock associations and degree of Alpine fabric development: 'Berger de la Sassa' and 'Bivouac de la Sassa'. The first subarea (Berger de la Sassa) comprises a gabbroic intrusive complex (Sassa metagabbros) only partially deformed during Alpine convergence. Deformation partitioning allowed the preservation of large coronitic domains in which the pre-Alpine igneous textures and intrusion relationships can be easily inferred. The second subarea (Bivouac de la Sassa) is characterized by AS metagranitoids with Alpine tectonitic or mylonitic textures, in which only rare mm- to m-sized coronitic domains occur. The degree of fabric evolution (Salvi et al., 2010) during Alpine deformation stages is represented on the map and on Figure 4 by different densities of foliation trajectories and by the shapes of igneous enclaves. Tectonitic fabrics mainly consist of secondary foliations (S-tectonites of Passchier & Trouw, 2005).

4.1. *Rock types*

Protoliths of mapped metaintrusive rocks consist of gabbros, leucogabbros, anorthosites, melanocratic gabbros, granitoids, tonalites, quartzdiorites, and porphyritic, plagiogranitic, and aplitic dykes (Figure 5a–h). The following synthetic description of different lithotypes is integrated with details on mineral composition and degree of Alpine fabric reworking (coronitic, tectonitic or mylonitic texture as represented in Figure 3) that are reported in Table 1.

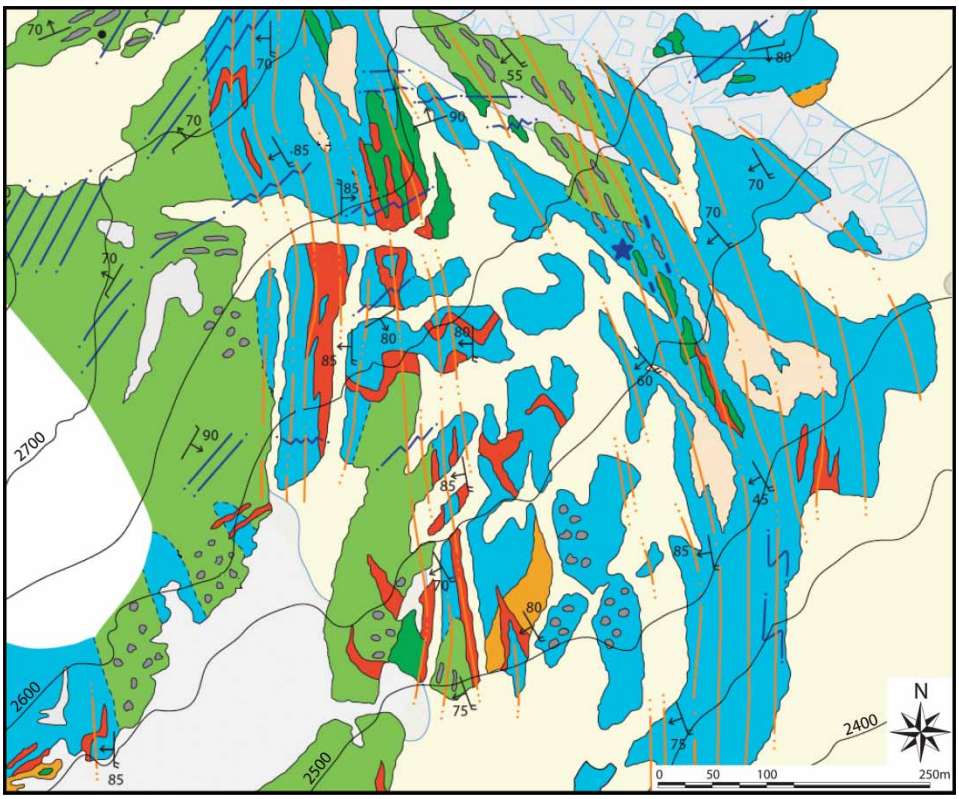

Figure 4. Detail of the map (southern sector of Berger de la Sassa subarea) showing hectometer-scale deformation partitioning: poorly deformed domains preserving the magmatic structures are wrapped by S1 or S2 foliated domains. Legend as in the 'Structural and petrographic map of the Sassa gabbro complex'.

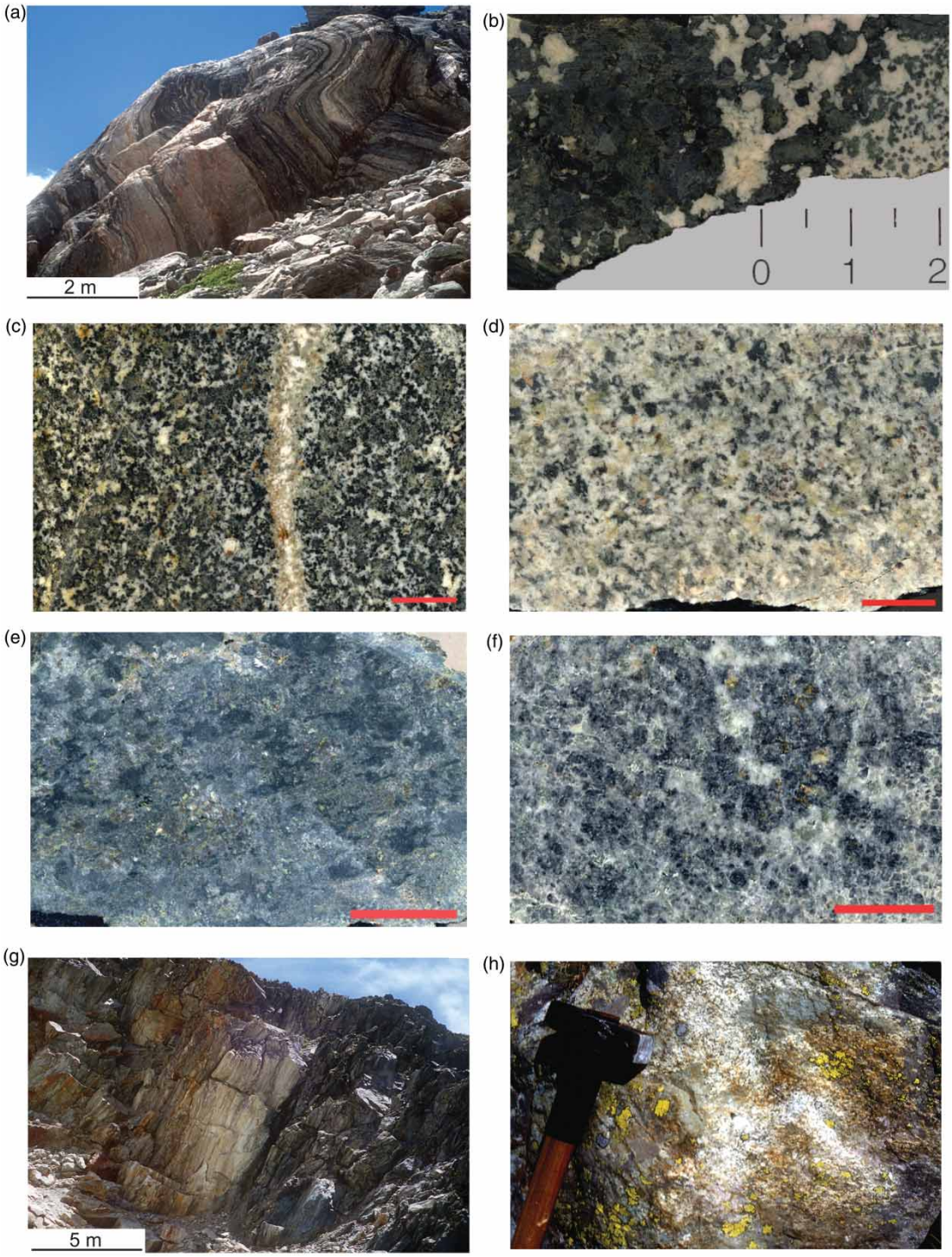

Figure 5. (a) leucocratic/melanocratic alternating layers (from cm- to m-thick) affected by D3 folds in metagranitoids; close to Bivouac de la Sassa; (b) mesocratic metagabbro with dark green clinopyroxene rimmed by dark amphibole, showing grain-size variation; scale bar in centimeters; (c) mm-grained metamorphic microgabbro cut by a meta-plagiogranitic vein with undulate contacts; red scale bar is 1 cm long; (d) mm-grained leucocratic metagabbro with less than 30% of amphibole and biotite content; red scale bar is 1 cm long; (e) melanocratic metagabbro mainly consisting of amphibole (dark green), opaque minerals, and chlorite (light green); red scale bar is 1 cm long; (f) mm-grained meta-anorthosite consisting of 95% of plagioclase (dark portions are fresh plagioclase grains); red scale bar is 1 cm long; (g) contact between metagabbros (deep green color) and meta-granitoids (yellowish color) is frequently marked by a thick mylonitic layer as in the case of upper Vallone d'Otemma; (h) meta-tonalite rich in porphyritic enclaves in Vallone d'Otemma.

4.1.1. *Acidic and intermediate protoliths (Arolla metagranitoids and meta-aplites)*

Acidic and intermediate rocks, belonging to AS metagranitoids, show a very heterogeneous texture and composition and three groups are recognized: leucocratic metagranitoids (Figure 5a), melanocratic metagranitoids, and meta-tonalites and −quartzdiorites. Textural features and mineral assemblages of different lithotypes are described in Table 1a.

4.1.2. *Basic protoliths (Sassa metaintrusives)*

Mesocratic gabbros, leucogabbros, melagabbros, and anorthosites constitute the Sassa mafic complex protoliths, which are intruded by porphyritic, plagiogranitic, and aplitic dykes. Fine-grained meta-plagiogranites occur in thin unmappable dykes and intruded the gabbros before Alpine deformation and metamorphism. Grain-size in mesocratic metagabbros (Figure 5b, c, microphotographs 6 and 7 on the map) varies from pegmatitic gabbros to microgabbros and they are rich in porphyritic enclaves. Leucocratic metagabbros (Figure 5d) are medium- to fine-grained rocks. Melanocratic metagabbros (Figure 5e) are medium- to fine-grained rocks and form m-sized

Table 1. Textural and mineralogical features of different lithotypes (a = acidic protoliths. b = basic protoliths) in the two mapped subareas.

Rock		**Coronitic**	**Tectonitic**	**Mylonitic**
Acidic and intermediate protoliths	*Leucocratic metagranitoids*		Minerals: quartz (20-40%), K-feldspar (20-40%), albite (10-20%), amphibole (0-10%), chlorite (10-30%), and white mica (10-20%). Spaced anastomosing foliation with microlithons of quartz, K-feldspar (augen-texture), and albite and films of white mica and chlorite. These films also wrap amphibole porphyroclasts, which are rimmed by chlorite. Locally igneous relic textures are preserved in m-sized domains.	Minerals: quartz (20-40%), K-feldspar (10-30%), albite (10-20%), chlorite (20-40%), and white mica (20-30%). Continuous foliation defined by quartz ribbons and shape preferred orientation (SPO) of chlorite and white mica. Locally quartz-feldspar layers mark this foliation and rare poorly deformed domains preserve K-feldspar porphyroclasts.
	Melanocratic metagranitoids			Minerals: chlorite (50-80%), amphibole (0-10%), epidote (0-10%), quartz (0-10%), and albite (0-10%). Mm-thick quartz layers and SPO of amphibole, chlorite, epidote, and albite define the foliation.
	Meta-tonalites and -quartzdiorites	Minerals: quartz (20-30%), plagioclase (30-40%), biotite (5-15%), and amphibole (10-30%). Plagioclase and quartz form mainly subhedral to anhedral crystals. Euhedral to subhedral black to deep green amphibole is associated with rare mm-sized biotite.		
	Meta-aplites	Minerals: quartz (50-60%), K-feldspar (40-50%), plagioclase (0-5%), and biotite (0-5%). Mm-sized subehdral quartz crystals are in equilibrium contact with euhedral K-feldspar crystals. Plagioclase forms fine-grained subhedral crystals. Biotite is interstitial between quartz and K-feldspar.	Minerals: quartz (50-60%), K-feldspar (30-40%), white mica (5-10%), biotite (0-2%), and chlorite (0-2%). Foliation in tectonites consists of quartz layers and SPO of rotated K-feldspar and biotite porphyroclasts and anastomosing white mica- and chlorite-bearing spaced films. K-feldspar is microboudinaged and chlorite overgrew biotite.	

(Continued)

Table 1. *(Continued)*

Rock		Coronitic	Tectonitic	Mylonitic
Basic protoliths	*Meta-plagiogranites*	Minerals: plagioclase (40-60%), quartz (40-60%), and biotite (0-10%). Plagioclase and quartz form subhedral crystals and biotite forms mm-sized euhedral crystals.		
	Mesocratic metagabbros	Minerals: plagioclase (40-70%), amphibole (10-50%), pyroxene (0-40%), biotite (0-5%), quartz (0-5%), and opaque minerals (0-2%). Plagioclase forms euhedral crystals and black amphibole is interstitial and rimmed by green amphibole. Biotite and quartz are interstitial between plagioclase and amphibole. Pyroxene forms aggregates or is enclosed in plagioclase (Fig. 5b)	Minerals: plagioclase (30-70%), amphibole (30-60%), chlorite (0-10%), white mica (0-5%), quartz (0-5%), and opaque minerals (0-2%); spaced foliation consisting of mm-sized amphibole- and plagioclase-bearing lithons and of anastomosing chlorite- and white mica- bearing films. Black to dark-brown amphibole shape preferred orientation (SPO) defines the foliation and single crystals are microboudinaged and rimmed by a deep green amphibole. Trails of green amphibole also defines the foliation films; these films wrap lenses of plagioclase aggregates. Locally quartz occurs in ribbons parallel to the foliation.	Minerals: amphibole (30-50%), white mica (20-30%), chlorite (20-30%), epidote (5-10%), quartz (0.5%), and opaque minerals (0.2%); foliation is pervasive and often defined by mm-thick layers of dark amphibole, chlorite and white mica. Generally amphibole is microboudinaged and necks are filled by bright green amphibole and chlorite. Locally thin quartz-layers are parallel to the foliation.
	Leucocratic metagabbros	Minerals: plagioclase (70-90%), amphibole (15-30%), biotite (0-10%), quartz (0-10%), and opaque minerals (0-1%); mm-sized euhedral to subhedral plagioclase crystals and the larger ones show compositional zoning. Fine-grained amphibole and biotite are interstitial between plagioclase grains and quartz is interstitial between plagioclase and amphibole.		
	Melanocratic metagabbros	Minerals: amphibole (20-25%), chlorite (20-25%), plagioclase (0-40%), biotite (0-5%) and opaque minerals (0-3%). Amphibole mainly forms anhedral and subhedral crystals surrounding relict microsites totally replaced by fine-grained aggregates of chlorite that could have been former olivine, ortopyroxene or Mg-spinel. Where chlorite is rare, amphibole forms euhedral crystals, plagioclase forms subhedral crystals surrounded by amphibole, rare mm-sized subhedral biotite is associated with amphibole.	Minerals: amphibole (40-60%), plagioclase (0-20%), chlorite (0-20%), epidote (10-20%), white mica (0-10%). and opaque minerals (0-3%); microlithons with dark amphibole, plagioclase, epidote, and chlorite and films with chlorite and minor white mica. Necks of microboudinaged amphibole are filled by greenish amphibole and chlorite.	Minerals: chlorite (70-90%), amphibole (10-30%), and opaque minerals (0-3%); foliation is defined by mm-sized chlorite, dark amphibole and fine-grained green amphibole. Generally dark amphibole is microboudinaged.
	Meta-anorthosites	Minerals: plagioclase (90-100%) and minor chlorite (0-10%); Dark grey plagioclase is euhedral to subhedral (Fig. 5f) and forms an adcumulitic texture. Chlorite occupies the intercumulus spaces and could be a replacement of mafic phases such as pyroxene and Mg-spinel.		
	Meta-porphyrites	Minerals: grey groundmass with amphibole (40-60%), plagioclase (40-60%), and biotite (0-10%) as phenocrysts; the porphyritic index is up to 20%.		

Table 2. Summary of the intrusion relationships in the Sassa gabbroic complex.

	melanocratic metagabbros	mesocratic metagabbros	leucocratic metagabbros	meta-anorthosites	meta-porphyrites Ia	meta-porphyrites Ib	meta-porphyrites II	meta-aplites	meta-plagiogranites
melanocratic metagabbros		melanocratic metagabbro lenses or layers with soft contacts in mesocratic metagabbros. Melanocratic metagabbro syndate or postdate mesocratic metagabbro	leucocratic metagabbro lenses or layers with soft contacts in melanocratic metagabbro				meta-porphyrites II cut melanocratic metagabbros	meta-aplites cut melanocratic metagabbros	Vein net in melanocratic metagabbros
mesocratic metagabbros	melanocratic metagabbro lenses or layers with soft contacts in mesocratic metagabbros. Melanocratic metagabbro syndate or postdate mesocratic metagabbro		amorphous bodies, lenses or layers of leucocratic metagabbro in mesocratic metagabbros or vice versa. The two rock types are contemporaneous	leucocratic metagabbro is the reaction rim between meta-anorthosites and mesocratic metagabbros	swarms of enclaves with or without preferential orientation showing soft or sawtooth shaped contacts within mesocratic metagabbros.	dykes with irregular and soft margins enclosing type Ia and often mesocratic metagabbro. They are syn-magmatic dykes	meta-porphyrites II cut mesocratic metagabbros	meta-aplites cut mesocratic metagabbros	veins and dykes in mesocratic metagabbros
leucocratic metagabbros	leucocratic metagabbro lenses or layers with soft contacts in melanocratic metagabbro	amorphous bodies, lenses or layers of leucocratic metagabbro in mesocratic metagabbros or vice versa. The two rock types are contemporaneous		lenses of anorthosites with gradual boundaries in leucocratic metagabbros			meta-porphyrites II cut leucocratic metagabbros	meta-aplites cut leucocratic metagabbros	
meta-anorthosites		leucocratic metagabbro is the reaction rim between meta-anorthosites and mesocratic metagabbros	lenses of anorthosites with gradual boundaries in leucocratic metagabbros				meta-porphyrites II cut meta-anorthosites	meta-aplites cut meta-anorthosites	

(*Continued*)

Table 2. *(Continued)*

	melanocratic metagabbros	mesocratic metagabbros	leucocratic metagabbros	meta-anorthosites	meta-porphyrites Ia	meta-porphyrites Ib	meta-porphyrites II	meta-aplites	meta-plagiogranites
meta-porphyrites Ia		swarms of enclaves with or without preferential orientation showing soft or sawtooth shaped contacts within mesocratic metagabbros.				in mesocratic metagabbros with soft contacts. Enclaves of porphyrites Ia concentrated at the margins. Often mesocratic metagabbros enclaves occur. Type Ia and Ib are coeval		meta-aplites cut meta-porphyrites Ia	
meta-porphyrites Ib		dykes with irregular and soft margins enclosing type Ia and often mesocratic metagabbro. They are syn-magmatic dykes			in mesocratic metagabbros with soft contacts. Enclaves of porphyrites Ia concentrated at the margins. Often mesocratic metagabbros enclaves occur. Type Ia and Ib are coeval			meta-aplites cut meta-porphyrites Ib	enclaves of foliated meta-plagiogranites in meta-porphyrites Ib
meta-porphyrites II	meta-porphyrites II cut melanocratic metagabbros	meta-porphyrites II cut mesocratic metagabbros	meta-porphyrites II cut leucocratic metagabbros	meta-porphyrites II cut meta-anorthosites				meta-porphyrites II cut meta-aplites	
meta-aplites	meta-aplites cut melanocratic metagabbros	meta-aplites cut mesocratic metagabbros	meta-aplites cut leucocratic metagabbros	meta-aplites cut meta-anorthosites	meta-aplites cut meta-porphyrites Ia	meta-aplites cut meta-porphyrites Ib	meta-porphyrites II cut meta-aplites		
meta-plagiogranites	Vein net in melanocratic metagabbros	veins and dykes in mesocratic metagabbros				enclaves of foliated meta-plagiogranites in meta-porphyrites Ib			

Table 3. Pre-Alpine and Alpine superposed structure and related mineral assemblages as inferred by microstructural analysis. Mineral abbreviations after Whitney and Evans (2010) except for white mica (Wm).

		pre-D1	D1	D2	D3
Berger de la Sassa subarea	Dominant rocks: melanocratic metagabbros (1), mesocratic metagabbros (2), leucocratic metagabbros (3), meta-plagiogranites (4), meta-anorthosites (5), meta-porphyrites (6)	**Igneous mesostructures:** cumulus stratification (cm-thick alternating Amp- and Pl-rich layers), subvertical lineation, and ESE and SW trending foliation. **Igneous assemblages: (**1) Cpx, Pl_I, Amp_I, Bt_I, Sp_I, Ilm, Ol-Opx?; (2) Pl_I, Cpx, Amp_I, Pl_{II}, Bt_I, Sp_I, Ilm, Opx?; (3) Pl_I, Cpx-Opx, Amp_I, Ttn, Ilm?; (4) Pl_I, Bt_I, Qtz; (5) Pl_I, Opx; (6) Pl_I, Amp_I, Bt_I, Qtz.	**Mesostructures**: S1 foliation locally mylonitic, up to m-sized tight to isoclinal folds and S-C structures. D1 deformation is concentrated along E-W trending sub-vertical bands. Deformation gradient increases from rim to core of these bands, where S1 foliation becomes mylonitic with S-C fabrics and intrafolial folds. S1 is spaced and anastomosing with microlithons constituted by Amp and Pl porphyroclasts and films of Wm and Chl. Amp porphyroclasts are microboudinaged and rimmed by green or blue-green Amp and Chl. S1 dips NW or SE with angles between 60°-90°; if transposed into S2, it dips SW; angle 70°-90°.	**Mesostructures**: S2 foliation locally mylonitic, mm- to m-sized tight to isoclinal folds. D2 deformation is concentrated in up to 100 m-thick NE-SW trending bands with gradient increasing inward and giving rise to a mylonitic foliation. Where D2 overprints D1, S1 is crenulated by mm-sized F2 folds (subvertical B2 axes) and S2 is a crenulation cleavage. Where D2 is more intense D1 structures and lithologic boundaries are transposed into S2. In this case F2 folds are m-sized with subvertical axial plane and axis. In mesocratic metagabbros S2 is a spaced foliation, with mm-thick Amp and Pl-bearing microlithons and anastomosing films marked by Chl, green Amp, and Wm. In melanocratic metagabbros S2 is a spaced foliation with Amp-bearing microlithons and anastomosing films marked by Chl, green Amp, and Ep. B2 axes dip with angles between 75° and 90° and S2 dips with angles between 65° and 90° toward ENE or WSW.	**Mesostructures**: S3 foliation, open folds with 10 meters wavelength. Where S1 and S2 foliations are more penetrative or mylonitic, mm- to cm-sized asymmetric D3 crenulation, locally associated to S3 foliation developed. S3 dips with an angle between 10° and 40° toward W. NE-SW trending axial plane and B3 axes are subhorizontal.
		Pre-Alpine metamorphic minerals (a= amphibolite facies conditions, b= greenschist facies conditions): (1a) Amp_{II} (Hbl), Bt_{II}; (1b) Amp_{III} (Act/Tr), Pl_{II} (Ab), Ep_I, Wm_I, Chl_I; (2a) Amp_{II} (Hbl), Pl_{IIa}; (2b) Amp_{III} (Act/Tr), Pl_{IIb}, Ep_I, Wm_I, Chl_I, Bt_{II}; (3b) Ep_I, Wm, Pl_{II}, Amp_{II}, Chl_I; (4b) Pl_{II}, Wm_I, Ep_I, Chl_I, Bt_{II}; (5b) Ep_I, Wm_I, Pl_{II}, Chl_I; (6a) Amp_{II} (Hbl) in type Ia and Ib; (6b) Ep_I, Wm_I, Pl_{II}, Amp_{III} (Act), Chl_I.	**Metamorphic minerals**: (1) coronitic and tectonitic fabrics: Amp_{IV} (Gln, Wnc), Ep_{II} (Czo), Chl_{II}, ± Tlc (in coronitic fabric); (2) tectonitic fabric: Amp_{IVa} (Gln, Wnc or Ts), Chl_{II}, Ep_{II} (Zo), ± Wm (Ph, Pg), ± Qtz, ± Rt; mylonitic fabric: Wm_{II} (Ph), Chl_{II}, Ep_{II} (Zo); coronitic fabric: Amp_{IV}, Ep_{II} (Zo). (3) coronitic fabric Ep_{II}, Rt; (5) coronitic fabric: Ep_{II}, Wm_{II}.	**Metamorphic minerals**: (1) tectonitic fabric: Amp_V (Act), Chl_{III}; mylonitic fabric: Amp_V (Act), Chl_{III}, Ep_{III} (Czo), Mag; coronitic Amp_V (Act), Chl_{III}, Ep_{III} (Fe-Ep); (2) tectonitic fabric: Amp_V (Act), Chl_{III}, Wm_{III}, Ep_{III}, Pl_{III}; coronitic fabric: Amp_V (Act), Chl_{III}, Wm_{III} (Ms), Ep_{III}, Ttn_{II}; (3) coronitic fabric: Amp_{III} (Tr-Act), Ttn_{II}; (4) coronitic and mylonitic fabrics: Chl_{II}, Wm_{II}, Ep_{II} (Czo), Qtz, Pl_{III} (Ab); (5) coronitic fabric: Ep_{III}.	**Metamorphic minerals**: no new mineral growth, dynamic re-crystallization, solution and passive rotation of syn-D2 minerals.

(*Continued*)

Table 3. *(Continued)*

		pre-D1	D1	D2	D3
Bivouac de la Sassa subarea	Dominant rocks: leucocratic metagranitoids (7), mesocratic metagranitoids (8), meta-tonalites and -quartzdiorites (9), meta-aplites (10)	**Igneous mesostructures:** cm- to dm-sized ellipsoidal to subspherical porphyritic enclaves (meta-tonalites, lower Vallone d'Otemma), more abundant at the tonalite-gabbro contact. Generally randomly oriented, locally SPO defining magmatic foliation.	**Mesostructures**: S1 foliation. In leucocratic metagranitoids S1 is a spaced foliation with Qtz- Fsp-bearing microlithons and anastomosing films marked by Wm and minor Chl; in the lithons Amp porphyroclasts are rimmed by Chl. Locally S1 is also marked by a layering of Qtz-Fsp-rich and phyllosilicate-rich layers. In mesocratic metagranitoids S1 is a continuous foliation defined by Chl, Amp, and Ep, wrapping Ab porphyroclasts. In meta-aplites faint S1 is defined by Wm and thin Qtz-layers, separating microlithons rich of Pl porphyroclasts. S1 dips with angles between 70° and 90° toward NW.	**Mesostructures:** S2 foliation generally mylonitic, isoclinal folds. D2 isoclinal folds have dm-sized wavelength and subvertical axial plane and axis. In leucocratic metagranitoids S2 is a spaced foliation. In melanocratic metagranitoids S2 is a continuous foliation defined by Qtz ribbons and SPO of Chl, Amp, and Ep wrapping rare mm-sized Ab porphyroclasts. In meta-tonalites and -diorites S2 is spaced and localized toward the boundary with leucocratic meta-granitoids. Westward dipping B2 axes show angles between 80° and 90°. S2 trends 120° to 180°N and 300° to 350°N and dips with angles between 45° and 90°.	**Mesostructures:** S3 spaced foliation, mm- to 10 m-scale open folds. S3 is more penetrative where pre-D3 fabric is mylonitic. S3 dips with angles between 0 and 35° toward SE and NE, F3 fold axis and axial surface are subhorizontal and trend NE-SW. F3 axis dips with angles between 5° and 30°.
		Igneous relics: (7) Amp_I (Hbl), Kfs, Pl_I, Qtz, Aln; (8) Pl_I, Qtz, Amp_I (Hbl), Kfs, Ilm, Spl; (9) Amp_I (Hbl), Bt_I; (10) Qtz, Kfs, Pl, Wm_I.	**Metamorphic minerals**: (7) Wm_I, Chl, Ep, blue-green Amp, Ttn, Qtz; (8) blue Amp; (9) blue Amp; (10) Wm_{II}, Ep_I.	**Metamorphic minerals**: (7) Wm_{II}, Chl_{II}, Qtz; (8) Chl, Wm, green Amp, ± Stp, ± Ttn; (9) Chl, Wm, green Amp, ± Stp, ± Ttn; (10) Wm_{II}, Chl.	**Metamorphic minerals:** (7) Wm_{III}, ± Chl_{III}, ± Ep_{II}, ± green Bt.

lenses within the leucocratic and mesocratic metagabbros. At Vallone d'Otemma meta-anorthosites (Figure 5f and photomicrograph 1 on the map) outcrop as m-sized lenses in leucogabbros and meta-porphyrites form dykes in basic meta-intrusives and in meta-tonalites/diorites, close to the contact with mesocratic metagabbro. Details on textures and variations in mineral compositions are listed in Table 1b.

5. Structural relationships

The two mapped subareas are characterized by different rock types and structures: (i) the Berger de la Sassa subarea with metagabbroic rocks weakly affected by the Alpine deformation and primary magmatic features detectable in

Figure 6. (a) metagabbro cut by meta-aplites and type II meta-porphyritic dykes. Porphyritic dykes show chilled margins. Black Brunton compass for scale; (b) S3 crenulation cleavage develops where S2 is more pervasive in mylonitic metagranitoids (Bivouac de la Sassa subarea); (c) View of the base of the Glacier de la Sassa. Valpelline Series and Arolla Series rocks are on the right side and left side of the picture respectively. The contact between the two Series is mylonitic, parallel to the S2 foliation recorded in the metagranitoids, and affected by meter-scale D3 folds; S2 trace in orange; (d) interference pattern between D2 and D3 folding in melanocratic metagranitoids; S1, S2, and AP3 are in blue, orange, and green, respectively; 4 cm long eraser as scale; (e) Ramsay's type 3 interference pattern between D2 and D3 folding in leucocratic metagranitoids; S1, S2, and AP3 are in blue, orange, and green, respectively.

Table 4. Summary of pre-Alpine and Alpine evolution from the magmatic emplacement of the Sassa gabbro to its final reworking during the Alpine cycle. A = amphibolite; GS = greenschist; BS = blueschist. Ages for magmatic emplacement are related to Matterhorn and Collon gabbro (Dal Piaz et al., 1977; Monjoie et al., 2005); D1 ages after Ayrton et al. (1982).

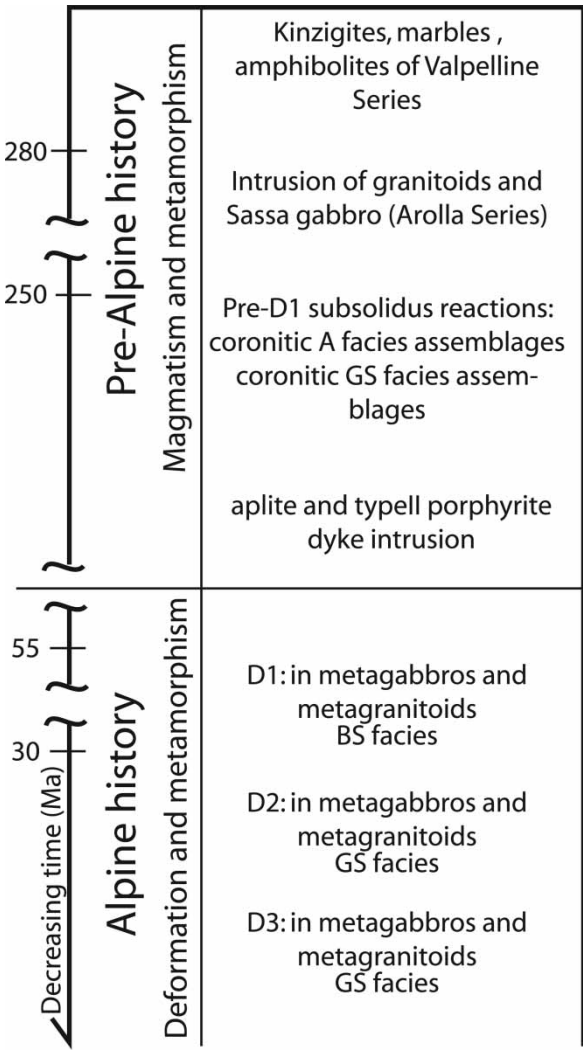

hectometer-sized volumes; (ii) the Bivouac de la Sassa subarea with metagranitoids pervasively affected by Alpine tectonitic and mylonitic textures.

The intrusion sequence can be inferred by the structural relations among different magmatic rocks (Table 2).

Hereafter we synthetically describe the pre-Alpine and Alpine structures in the two subareas; a more detailed description is given in Table 3, where the complete list of superposed structures and the mineral support of successive fabrics are itemized.

5.1. *Berger de la Sassa subarea*

5.1.1. *Pre-Alpine magmatic structures*

The contact between metagabbros and metagranitoids is regularly marked by a thick mylonitic band, affecting both rock types (Figure 5g and panoramic photo 2 on the map).

Mesocratic metagabbros are prevalent and contain melanocratic m-sized tabular or lenticular layers with transitional contacts. Meta-plagiogranites and pegmatitic metagabbros form ramified vein and dykelet nets within both

metagabbros. The soft contact between meta-plagiogranitic veins, pegmatitic metagabbro dykes, and mesocratic metagabbros suggests that the former represent residual melts that were injected into the embodying material when it was still a viscous crystal mush.

Three types of meta-porphyrites have been distinguished: (i) type Ia are enclosed in mesocratic metagabbros; enclaves are stretched and concentrated in m-thick layers, defining a magmatic foliation; (ii) type Ib meta-porphyrites form m-thick dykes, which are disrupted within mesocratic metagabbros, displaying a soft contact with them (outcrop photo 4 on the map). These dykes contain enclaves of the country rock. Porphyrite enclaves in the country rock are concentrated at the dyke margins; (iii) type II meta-porphyrites of Vallone d'Otemma form 10 cm-thick dykes sharply intruding metagabbros and meta-aplites and locally showing chilled margins (Figure 6a and outcrop photo 1 on the map). These features suggest that type Ia and Ib porphyrites intruded a gabbro crystal mush, whereas type II was emplaced in totally solidified country rocks.

Except for type II porphyrites and meta-aplites, all of these rocks underwent pre-Alpine subsolidus re-equilibrations under amphibolite facies conditions (Table 3), followed by greenschist re-equilibration. The lack of subsolidus pre-Alpine amphibolite facies mineral assemblages in type II porphyrites and meta-aplites, together with their sharp intrusive contacts and chilled margins, suggests that these two kinds of dykes intruded the country rocks at the end of the pre-Alpine evolution.

5.1.2. *Alpine tectonic structures*

D1 deforms and transposes all the magmatic contacts and features, including aplitic and type II porphyritic dykes, and is concentrated along E-W trending sub-vertical bands. The foliation intensity gradient increases from the rim to the core of these deformation bands, where the S1 foliation is mylonitic. S1 is generally a spaced foliation; where it is mylonitic, boundaries of dykes are transposed and metaporphyritic enclaves are elongated and boudinaged (outcrop photos 5 and 10 on the map).

D2 structures are not pervasive in metagabbros and D2 is concentrated in NE-SW trending bands in which S2 foliation may be mylonitic (photomicrographs 2 and 8 on the map). F2 folds show subvertical B2 axes and are associated with S2 crenulation cleavage (outcrop photo 6 on the map). D1 structures and lithologic boundaries may be isoclinally folded (outcrop photo 3 on the map) and transposed into S2. In the upper Vallone d'Otemma, the contact between melanocratic metagabbros and leucocratic metagranitoids is defined by a pervasive S2 mylonitic foliation (panoramic photo 2 on the map), which dips 45° toward the NNE.

D3 structures consist of open folds with tens of meters wavelength. Where foliations S1 and S2 are more penetrative or mylonitic, mm- to cm-sized asymmetric D3 crenulation, locally associated with a differentiated new mineral layering (S3), developed.

In the upper Vallone d'Otemma the boundary between metagabbros and metagranitoids shows a sinistral offset of tens of meters and in its central part, meta-leucogabbro and meta-anorthosite layers show the same offset, suggesting that a *fault* is buried by talus and glacial deposits.

5.2. *Bivouac de la Sassa subarea*

5.2.1. *Pre-Alpine magmatic structures*

Magmatic structures are basically preserved only in meta-tonalites and -quartzdiorites as the cm- to dm-sized porphyritic enclaves (photomicrograph 3 on the map) in the lower Vallone d'Otemma (more abundant toward the boundary with metagabbro). Contact between leucocratic and melanocratic metagranitoids and between meta-aplites and country rocks are generally parallelized to S1 or S2.

5.2.2. *Alpine tectonic structures*

In metagranitoids S1 frequently transposes lithologic boundaries and is in small-scale relics. In leucocratic metagranitoids S1 is a spaced foliation, in melanocratic metagranitoids it is a continuous foliation whereas in meta-aplites it is only locally preserved.

D2 are the most pervasive structures and partially or fully obliterate previous structures. S2 varies from a spaced to mylonitic foliation and frequently is a subvertical transposition foliation, generally associated with isoclinal F2 folds (outcrop photo 8 on the map) with subvertical axis.

D3 structures are pervasive and produce asymmetric folds where previous fabrics are more evolved (photomicrograph 5 on the map and Figure 6b) and S3 crenulation cleavage (photomicrograph 4 on the map) mainly developed in mylonitic leucocratic metagranitoids; F3 open folds display a 10-meter scale wavelength (Figure 6c and panoramic photos 7 and 10 on the map). In Lower Bec de la Sassa area Ramsay's type 2 and 3 overprinting patterns result by the superposition of F2 and F3 folds (Figures 6d, e).

Microstructural analysis of different lithotypes from both subareas (Table 3) indicates that mineral associations supporting S1 foliation developed under blueschist facies conditions, whereas S2 and S3 are marked by greenschist facies minerals.

6. Summary and conclusions

This detailed structural and petrographic mapping facilitated the reconstruction of the deformation and metamorphic history of DBN throughout the removal of the Alpine tectonic imprints back to a few undeformed igneous-textured cores of Permian gabbros and granitoids.

Strain partitioning during Alpine deformation allows the identification of domains where the magmatic features are still well preserved, even though igneous minerals are replaced by pre-Alpine or Alpine metamorphic minerals (e.g., south of Berger de la Sassa, at the lower southeast slope of Grand Epicoune, and in the central part of Vallone d'Otemma). Where the Alpine deformation is weak, the analysis of intersection relationships between the different magmatic rocks (Table 2) allowed us to infer the pre-Alpine magmatic history: the Sassa complex is the result of multiple intrusions of heterogeneous gabbroic magmas at intermediate crustal levels; however, sharp dyke contacts and chilled margins testify that protoliths of type II meta-porphyrites and meta-aplites emplaced at shallow crustal levels, into the main gabbro body when this was totally crystallized. Pre-Alpine coronitic textures developed under amphibolite and later greenschist facies metamorphic conditions replacing magmatic assemblages.

Within gabbroic rocks, S1 foliation dominates east of Berger de la Sassa, whereas northwest of Berger de la Sassa and in the upper Vallone d'Otemma, S1 is preserved only in the S2 lithons. Between Berger de la Sassa and the lower southeast slope of Grand Epicoune, S2 obliterates S1, rotating and transposing dykes and magmatic contacts. Generally S2 is localized in shear zones at the boundaries between gabbros and metagranitoids and along bands crosscutting the gabbro. S3 foliation is the less pervasive and is recorded mainly where D1 and D2 deformation-enhanced mineral transformations generated phyllosilicate richer rocks (lower part of Vallone d'Otemma and Bivouac de la Sassa).

This analytical field approach supports a more objective link of the time sequence of mineral re-equilibrations with fabric evolution. In particular, this study allowed the discrimination of geologic traces related to the pre-Alpine magmatic and post-magmatic evolution and Alpine history as synthesized in the sequence of geologic events in Table 4. The pre-Alpine metamorphic coronitic mineral assemblages suggest a decompression during the cooling of the Sassa gabbro complex. The Alpine history is characterized by the localization of deformation within metagabbros and metagranitoids during both subduction and exhumation as testified by blueschist facies mineral assemblages marking S1 in metagabbros and by the syn-D2 and -D3 mineral assemblages characteristic of greenschist facies conditions.

Software

The Sassa geological map used a topographic base (the CTR – Technical Regional Topography) provided by the Val d'Aosta Regional Administration. The projection coordinate system is UTM ED50; the original 1:10,000-scale was enlarged up to 1:2500 to increase the mapping detail. The map presents a synthesis of the whole data set at a scale of 1:2500 on a redrawn original topographic base. Graphical representation was performed using Adobe Illustrator. The map plate displays equal area lower hemisphere Schmidt projections (StereoWinFull120; Allmendinger, 2002) of superposed fabric elements, such as tectonic (S1, S2, S3) and magmatic foliations, fold axes (B2, B3), and magmatic lineations (n = number of measurements). Meso- and microstructures of the most significant stages of the geological history of the analyzed area are shown in pictures on the map.

Acknowledgements

R. Berg, C. Malatesta, and M. Shand are thanked for the accurate revisions. C. Malinverno provided thin sections. M. Zucali, G. Rebay, and M. Roda are thanked for stimulating discussions. Funding by PRIN 2008 'Tectonic trajectories of subducted lithosphere in the Alpine collisional orogen from structure, metamorphism and lithostratigraphy'. D.Z. acknowledges funding from the project: 'Studio petrologico e strutturale delle rocce di alta pressione delle Alpi Occidentali', Università di Pavia.

References

Allmendinger, R.W. (2002), StereoWinFull120 for Windows. Retrieved May 2011, from http://www.wuala.com/GeologiaUWR/Tektonika/StereoWinFull120.zip?lang=it.

Argand, E. (1911). Les nappes de recouvrement des Alpes pennines et leurs prolongements structuraux [The overthrust nappes of Penninic Alps and their structural prolongations]. *Materiaux pour la Carte Géologique de la Suisse*, (n.s.), 1–26.

Austrheim, H. (1990). The granulite-eclogite transition: A comparison of experimental work and a natural occurence in the Bergen Arcs, western Norway. *Lithos*, *25,* 163–169. doi: 10.1016/0024-4937(90)90012-P.

Ayrton, S., Bugnon, C., Haarpainter, T., Weidmann, M., & Frank, E. (1982). Geologie du front de la nappe de la Dent Blanche dans la region des Monts-Dolins, Valais [Geology of the Dent Blanche nappe front in the region of Monts-Dolins, Valais]. *Eclogae Geologicae Helvetiae*, *75,* 269–286.

Burri, M., Alliman, M., Chessex, R., Dal Piaz, G.V., Della Valle, G., Du Bois, L., Gouffon, Y., Guermani, A., Hagen, D., Krummenacher, D., & Looser, M.-O. (1998). Atlas Géologique de la Suisse 1:25000, feuille 1346 Chanrion avec partie nord de la feuille 1366 Mont Vélan [Geological Atlas of Switzerland 1:25,000 scale, sheet 1346 Chanrion with the northern part of sheet 1366 Mont Velan]. Office fédéral de topographie.

Bussy, F., Venturini, C., Hunziker, J., & Martinotti, G. (1998). U-Pb ages of magmatic rocks of the Western Austroalpine Dent Blanche-Sesia Unit. *Schweizerische Mineralogische und Petrographische Mitteilungen*, *78,* 163–168.

Canepa, A., Castelletto, M., Cesare, B., Martin, S., & Zaggia, L. (1990). The Austroalpine Mont Mary nappe (Italian Western Alps). *Memorie di Scienze Geologiche*, *42,* 1–17.

Ciarapica, G., Dal Piaz, G.V., & Passeri, L. (2010). Late Triassic microfossils in the Roisan zone, Austroalpine Dent Blanche-Mont Mary nappe system, NW-Alps. *Rendiconti online della Società Geologica Italiana*, *11,* 259–260.

Compagnoni, R., Dal Piaz, G.V., Hunziker, J.C., Gosso, G., Lombardo, B., & Williams, P.F. (1977). The Sesia-Lanzo Zone: A slice of continental crust, with alpine HP-LT assemblages in the Western Italian Alps. *Società Italiana di Mineralogia e Petrologia*, *33,* 281–334.

Connors, K.A., & Lister, G.S. (1995). Polyphase deformation in the western Mount Isa Inlier, Australia: Episodic or continuous deformation? *Journal of Structural Geology*, *17*(3), 305–328. doi: 10.1016/0191-8141(94)00057-7.

Dal Piaz, G.V. (1993). Evolution of Austroalpine and Upper Penninic basement in the Northwestern Alps from Variscan convergence to post-Variscan extension. In J. Von Raumer & F. Neubauer (Eds.), *Pre-Mesozoic geology in the Alps* (pp. 325–342). Berlin: Springer-Verlag.

Dal Piaz, G.V. (1999). The Austroalpine-Piedmont nappe stack and the puzzle of Alpine Tethys. *Memorie di Scienze Geologiche, Padova*, *51,* 155–176.

Dal Piaz, G.V., De Vecchi, G., & Hunziker, J.C. (1977). The Austroalpine layered gabbros of the Matterhorn and Mt. Collon-Dents de Bertol. *Schweizerische Mineralogische und Petrographische Mitteilungen*, *57,* 59–88.

Dal Piaz, G.V., Hunziker, J.C., & Martinotti, G. (1972). La Zona Sesia - Lanzo e l'evoluzione tettonico-metamorfica delle Alpi Nordoccidentali interne [The Sesia - Lanzo Zone and the tectono-metamorphic evolution of the internal North-western Alps]. *Memorie della Società Geologica Italiana*, *11,* 433–460.

Diehl, E.A., Masson, R., & Stutz, A.H. (1952). Contributo alla conoscenza del ricoprimento Dent Blanche [Contribution to the knowledge of the Dent Blanche nappe]. *Memorie degli Istituti di Geologia e Mineralogia dell'Università di Padova*, *17,* 5–52.

Ernst, W.G., & Liou, J.G. (2008). High- and ultrahigh-pressure metamorphism: Past results and future prospects. *American Mineralogist*, *93,* 1771–1786. doi: 10.2138/am.2008.2940.

Gardien, V., Reusser, E., & Marquer, D. (1994). Pre-Alpine metamorphic evolution of the gneisses from the Valpelline Series (Western Alps, Italy). *Schweizerische Mineralogische und Petrographische Mitteilungen*, *74,* 489–502.

Gosso, G., Brizio, D., Deregibus, C., Eusebio, A., Gallo, M., Rattalino, E., Rossi, F., & Tosetto, S. (1983). Due cinematiche possibili per la coppia di falde Brianzonese ligure- Flysch a Elmintoidi [Two possible kinematics for the Ligurian Briançonnais and Helminthoid Flysch nappes]. *Memorie Società Geologica Italiana*, *26,* 463–472.

Gosso, G., Messiga, B., Rebay, G., & Spalla, M.I. (2010). Interplay between deformation and metamorphism during eclogitization of amphibolites in the Sesia-Lanzo Zone of the Western Alps. *International Geology Review*, *52*(10), 1193–1219. doi: 10.1080/00206810903529646.

Hobbs, B.E., Ord, A., Spalla, M.I., Gosso, G., & Zucali, M. (2010). The interaction of deformation and metamorphic reactions. *Geological Society, London, Special Publications*, *332,* 189–223. doi: 10.1144/SP332.12.

Johnson, S.E., & Duncan, A.C. (1992). Fault identification in complexly deformed schist terrains: Examples from the USA and Australia. *Tectonophysics*, *216,* 291–308. doi: 10.1016/0040-1951(92)90402-R.

Kienast, J.R., & Nicot, E. (1971). Presence d'une paragenese a disthene et chloritoide (d'age alpin probable) dans les gneiss a sillimanite, grenat et cordierite de Valpelline (Val d'Aoste, Italie) [Occurrence of a kyanite- chloritoid assemblage (likely of alpine age) in the Valpelline sillimanite-garnet-cordierite gneisses (Val d'Aosta, Italy)]. *Compte Rendu Academie des Sciences Paris, D*, *272,* 1836–1839.

Lardeaux, J.M., & Spalla, M.I. (1990). Tectonic significance of P-T-t paths in metamorphic rocks: Examples from ancient and modern orogenic belts. *Memorie della Società Geologica Italiana*, *45,* 51–69.

Lardeaux, J.M., & Spalla, M.I. (1991). From granulites to eclogites in the Sesia zone (Italian Western Alps): A record of the opening and closure of the Piedmont ocean. *Journal of Metamorphic Geology*, *9,* 35–59. doi: 10.1111/j.1525-1314.1991.tb00503.x.

Manzotti, P. (2011). Petro-structural map of the Dent Blanche tectonic system between Valpelline and Valtournenche valleys, Western Italian Alps. *Journal of Maps*, *2011,* 340–352. doi: 10.4113/jom.2011.1179.

Marotta, A.M., Spalla, M.I., & Gosso, G. (2009). Upper and lower crustal evolution during lithospheric extension: Numerical modelling and natural footprints from the European Alps. In U. Ring & B. Wernicke (Eds.), Extending a continent: Architecture rheology and heat budget. *Geological Society, London, Special Publications, 321*, 33–72.

Meda, M., Marotta, A.M., & Spalla, M.I. (2010). The role of mantle hydration into continental crust recycling in the wedge region. In M.I. Spalla, A.M. Marotta, & G. Gosso (Eds.), Advances in interpretation of geological processes: Refinement of multi-scale data and integration in numerical modelling. *Geological Society, London, Special Publications, 332*, 149–172.

Monjoie, P., Bussy, F., Lapierre, H., & Pfeifer, H.R. (2005). Modeling of in-situ crystallization processes in the Permian mafic layered intrusion of Mont Collon (Dent Blanche nappe, western Alps). *Lithos*, *83,* 317–346. doi: 10.1016/j.lithos.2005.03.008.

Passchier, C.W., Myers, J.S., & Kröner, A. (1990). *Field geology of high-grade gneiss terrains*. Berlin: Springer Verlag. doi: 10.1007/978-3-642-76013-6.

Passchier, C.W., & Trouw, R.A.J. (2005). *Microtectonics*. Berlin, Heidelberg, New York: Springer.

Pennacchioni, G., & Guermani, A. (1993). The mylonites of the Austroalpine Dent Blanche nappe along the northwestern side of the Valpelline valley (Italian Western Alps). *Memorie di Scienze Geologiche*, *45,* 37–55.

Polino, R., Dal Piaz, G.V., & Gosso, G. (1990). Tectonic erosion at the Adria margin and accretionary processes for the Cretaceous orogeny of the Alps. *Memoir de la Societé Géologique Française*, *156,* 345–367.

Rebay, G., & Spalla, M.I. (2001). Emplacement at granulite facies conditions of the Sesia-Lanzo metagabbros: An early record of Permian rifting? *Lithos*, *58,* 85–104. doi: 10.1016/S0024-4937(01)00046-9.

Roda, M., & Zucali, M. (2008). Meso and microstructural evolution of the Mont Morion metaintrusive complex (Dent-Blanche nappe, Austroalpine domain, Valpelline, Western Italian Alps). *Bollettino della Società Geologica Italiana (Italian Journal of Geoscience)*, *127*(1), 1–19.

Roda, M., & Zucali, M. (2011). Tectono-metamorphic map of the Mont Morion Permian metaintrusives (Mont Morion - Mount Collon - Matterhorn Complex, Dent Blanche Unit), Valpelline - Western Italian Alps. *Journal of Maps*, *2011,* 519–535. doi: 10.4113/jom.2011.1194.

Salvi, F., Spalla, M.I., Zucali, M., & Gosso, G. (2010). 3D-evaluation of fabric evolution and metamorphic reaction progress in polycyclic and polymetamorphic terrains: A case from the Central Italian Alps. *Geological Society, London, Special Publications*, *332,* 173–187. doi: 10.1144/SP332.11.

Spalla, M.I., Gosso, G., Marotta, A.M., Zucali, M., & Salvi, F. (2010). Analysis of natural tectonic systems coupled with numerical modelling of the polycyclic continental lithosphere of the Alps. *International Geology Review*, *52*(10–12), 1268–1302. doi: 10.1080/00206814.2010.482737.

Spalla, M.I., Lardeaux, J.M., Dal Piaz, G.V., Gosso, G., & Messiga, B. (1996). Tectonic significance of alpine eclogites. *Journal of Geodynamics*, *21*(3), 257–285. doi: 10.1016/0264-3707(95)00033-X.

Spalla, M.I., Siletto, G.B., Di Paola, S., & Gosso, G. (2000). The role of structural and metamorphic memory in the distinction of tectono-metamorphic units: The basement of the Como Lake in the Southern Alps. *Journal of Geodynamics*, *30,* 191–204. doi: 10.1016/S0264-3707(99)00033-2.

Spalla, M.I., Zanoni, D., Williams, P.F., & Gosso, G. (2011). Deciphering cryptic P-T-d-t histories in the western Thor-Odin dome, Monashee Mountains, Canadian Cordillera: A key to unravelling pre-Cordilleran tectonic signatures. *Journal of Structural Geology*, *33,* 399–421. doi: 10.1016/j.jsg.2010.11.014.

Spalla, M.I., Zucali, M., Di Paola, S., & Gosso, G. (2005). A critical assessment of the tectono-thermal memory of rocks and definition of tectono-metamorphic units: evidence from fabric and degree of metamorphic transformations. In D. Gapais, J.P. Brun, & P. Cobbold (Eds.), Deformation mechanisms, rheology and tectonics: From minerals to the lithosphere. *Geological Society London, Special Publications, 243*, 227–247.

Stutz, A.H., & Masson, R. (1938). Zur tektonik der Dent Blanche Decke [About the tectonics of the Dent Blanche nappe overthrust]. *Schweizerische Mineralogische und Petrographische Mitteilungen*, *18,* 929–955.

Venturini, G., Martinotti, G., Armando, G., Barbero, M., & Hunziker, J. (1994). The central Sesia-Lanzo Zone (Western Italian Alps): New field observations and lithostratigraphic subdivisions. *Schweizerische Mineralogische und Petrographische Mitteilungen*, *74,* 115–125.

Vuichard, J.P. (1989). *La marge Austroalpine durant la collision alpine: evolution tectonometamorphique de la Zone Sesia-Lanzo* [The Austroalpine margin during the Alpine collision: tectono-metamorphic evolution of the Sesia- Lanzo Zone]. Unpublished Thèse de Doctorat, Rennes.

Whitney, D.L., & Evans, B.W. (2010). Abbreviations for names of rock-forming minerals. *American Mineralogist*, *95,* 185–187. doi: 10.2138/am.2010.3371.

Williams, P.F. (1985). Multiply deformed terrains - problems of correlation. *Journal of Structural Geology*, *7*(3/4), 269–280. doi: 10.1016/0191-8141(85)90035-5.

Zanoni, D. (2010). Structural and petrographic analysis at the north-eastern margin of the Oligocene Traversella pluton (Internal Western Alps, Italy). *Bollettino della Società Geologica Italiana (Italian Journal of Geoscience)*, *129*(1), 51–68.

Zanoni, D., Spalla, M.I., & Gosso, G. (2010). Structure and PT estimates across late-collisional plutons: Constraints on the exhumation of Western Alpine continental HP units. *International Geology Review*, *52,* 1244–1267. doi: 10.1080/00206814.2010.482357.

Zucali, M., Spalla, M.I., & Gosso, G. (2002). Fabric evolution and reaction rate as correlation tool: The example of the Eclogitic Micaschists complex in the Sesia-Lanzo Zone (Monte Mucrone – Monte Mars, Western Alps Italy). *Schweizerische Mineralogische und Petrographische Mitteilungen*, *82,* 429–454.